PHYSICAL REVIEW B VOLUME 58, NUMBER 20 15 NOVEMBER 1998-II

Optical spectroscopy of charge-ordering transition in $La_{1/3}Sr_{2/3}FeO_3$

T. Ishikawa, S. K. Park, T. Katsufuji, T. Arima,* and Y. Tokura
Department of Applied Physics, University of Tokyo, Tokyo 113-8656, Japan
(Received 19 June 1998; revised manuscript received 14 August 1998)

The change of the electronic structure and lattice dynamics upon the charge-ordering (CO) transition has been investigated for a $La_{1/3}Sr_{2/3}FeO_3$ crystal by measurements of optical spectra. The CO transition, as characterized by sequential 2:1 ordering of nominal Fe^{3+} and $Fe^{5+}(111)_c$ sheets at $T_{CO}=198$ K, activates several additional optical phonon modes due to the charge modulation and opens an optical gap (up to $2\Delta\sim0.13$ eV). The spectral intensity of the activated phonon mode shows a discontinuous increase at T_{CO} reflecting the first-order nature of the CO transition. By contrast, the optical gap value increases rather continuously with decreasing temperature below T_{CO}, implying the effect of the concomitant antiferromagnetic spin ordering on the gap magnitude and structure. [S0163-1829(98)51542-1]

Transition metal oxides (TMO's) have recently been investigated extensively in the light of the metal-insulator transition relevant to electron correlations.[1] Among various electronic phase transitions, the charge ordering (CO) transition is widely seen in many TMO's with commensurate hole doping, such as the $x=\frac{1}{8}$ anomaly of the high-temperature superconducting cuprates,[2] colossal-magnetoresistive manganites ($x=\frac{1}{2}$),[3,4] layered nickelates ($x=\frac{1}{3}$),[5,6] and layered manganites ($x=\frac{1}{2}$).[7] Undoubtedly, the intersite coulomb repulsion is one of the driving forces for the CO transition. Verwey transition in magnetite (Fe_3O_4) is one such example,[8] in which Fe^{2+} and Fe^{3+} with almost full spin-polarization are ordered at the B site of the spinel structure below $T_V\sim120$ K. In most other cases, however, the magnetic interaction seems to be also responsible for stabilization of the charge-ordered state. The CO transition in most of the TMO's shows up by accompanying the antiferromagnetic spin correlation as well as the concomitant lattice distortion.[1]

We spectroscopically investigate this charge-ordered state in a $La_{1-x}Sr_xFeO_3$ ($x=\frac{2}{3}$) crystal. The first panel of Fig. 1 shows the temperature dependence of resistivity. The value of resistivity is fairly low at room temperature, being reminiscent of metallic nature, and slightly increases with decreasing the temperature. At the CO transition temperature ($T_{CO}=198$ K), resistivity shows abrupt increase, while the magnetization shows a cusp structure (the second panel of Fig. 1), corresponding to the transition from a paramagnetic metallic state to an antiferromagnetic CO state. The CO transition of this compound has been assigned to the ordering of magnetically different Fe sites, i.e., the nominal Fe^{3+} ($3d^5$) and Fe^{5+} ($3d^3$) sites with the ratio of 2:1 by measurements of Mössbauer spectra (Ref. 9) and magnetic neutron diffraction.[10] More lately, the structural modulation accompanying the CO transition has been confirmed by the electron microscopy.[11] The CO pattern of this compound was shown in the inset of Fig. 2. Layers of nominal Fe^{3+} and Fe^{5+} ions are ordered in the sequence $\ldots533533\ldots$ along the pseudocubic $[111]_c$ direction, or along the rhombohedral z direction. Thus, the valence-skipping charge-ordered state in $La_{1/3}Sr_{2/3}FeO_3$ may be viewed as a condensation of the hole bipolarons (Fe^{5+}, $3d^3$) in the magnetic background of Fe^{3+} ($3d^5$) lattice. In reality, the p-hole character of the nominal Fe^{5+} species is significant,[12] yet the breathing-type distortion of the FeO_6 octahedron should couple with the charge modulation. In this paper, we show the result of the optical measurement of this compound, and argue the effect of the CO on the electronic structure and lattice dynamics.

Crystals of $La_{1-x}Sr_xFeO_3$ ($x=\frac{2}{3}$) were melt grown by the floating zone method. The details of the crystal growth and the structural characterization will be reported elsewhere.[13] Temperature dependencies of resistivity and magnetic susceptibility of the same crystal as used in the following optical measurements are readily shown in the upper two panels of Fig. 1. Near-normal-incidence reflectivity spectra were measured on a crystal with a typical size of 6 mm$\phi\times$2 mm,

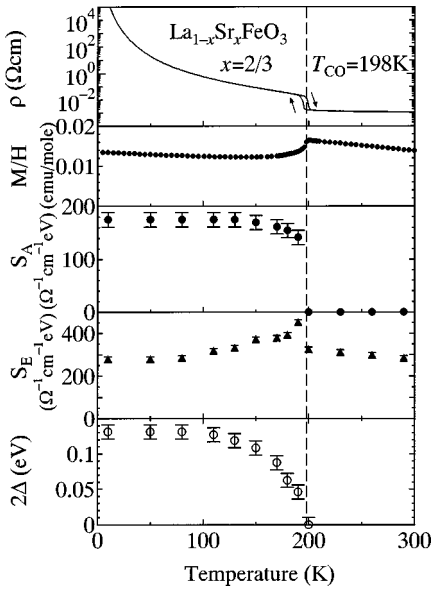

FIG. 1. Temperature dependence of various physical quantities for a $La_{1-x}Sr_xFeO_3$ ($x=\frac{2}{3}$) crystal. The top panel: the resistivity ρ; the second panel: the magnetization M at $\mu_0H=1$ T; the third panel: the oscillator strength (S_A) of the activated Fe-O stretching phonon mode at 0.08 eV (see Fig. 3 and text); the forth panel: the oscillator strength (S_E) of the Fe-O stretching phonon mode at 0.07 eV (see Fig. 3 and text); the bottom panel: the optical gap 2Δ estimated by an extrapolation procedure (see Fig. 4 and text).

 ©1998 The American Physical Society

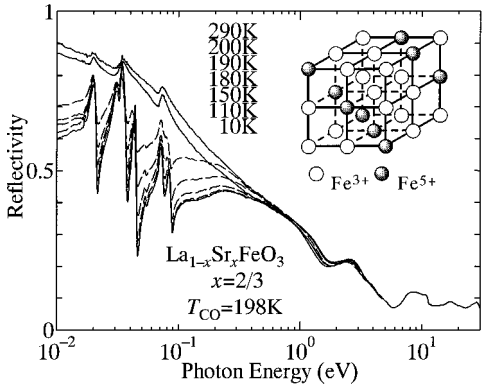

FIG. 2. Temperature dependence of the reflectivity spectra for a $La_{1-x}Sr_xFeO_3$ ($x=\frac{2}{3}$) crystal with the charge ordering transition temperature $T_{CO}=198$ K. Solid lines represent the spectra at 10 K, 200 K (just above T_{CO}), and 290 K. The inset shows the charge ordering model (Refs. 9–11) for this compound.

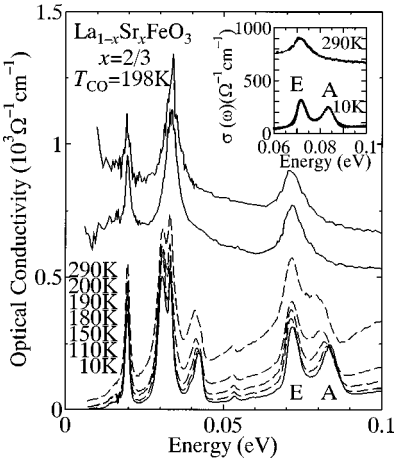

FIG. 3. Temperature dependence of the optical conductivity spectra in the optical phonon region (<0.1 eV) for a $La_{1-x}Sr_xFeO_3$ ($x=\frac{2}{3}$) crystal with the charge ordering temperature $T_{CO}=198$ K. Solid lines represent the spectra at 10 K, 200 K (just above T_{CO}), and 290 K. The inset shows spectra at 290 K and 10 K with each Lorentzian-fit curve (see text).

the surface of which was specularly polished with alumina powder. We used Fourier spectroscopy for the photon energy range of 0.008–0.8 eV and the grating spectroscopy for 0.6–36 eV. For the higher-energy (>5 eV) measurements at room temperature, the synchrotron radiation at INS-SOR, Institute for Solid State Physics, University of Tokyo, was utilized as a light source. The temperature dependence of the reflectivity spectra was measured for 0.008–5 eV. Since the temperature dependence of the spectra were essentially not discernible above 4 eV, the room-temperature data above 5 eV were connected to perform the Kramers-Kronig (KK) analysis and deduce the optical conductivity spectra at respective temperatures. For the analysis, we assumed the constant reflectivity below 0.01 eV and ω^{-4} extrapolation above 36 eV. Variation of the extrapolation procedures below 0.01 eV was confirmed to cause negligible difference for the calculated conductivity spectra above 0.02 eV.

Figure 2 shows the temperature dependence of the reflectivity spectra. The structures of spectra below 5 eV are mainly composed of charge transfer (CT) type transition between Fe $3d$ and O $2p$ states; namely, the transitions with the final states of $t_{2g\uparrow}^3 e_{g\uparrow}^2$ for below 2 eV and of $t_{2g\uparrow}^3 t_{2g\downarrow}^1 e_{g\uparrow}^1$ for around 3 eV. The reflectivity value increases toward unity with decreasing photon energy at temperatures above T_{CO}, indicating metallic nature. Once the temperature is decreased below T_{CO}, the reflectivity value in a low energy region (below 0.7 eV) is abruptly suppressed and the shape of the spectrum shows an insulating feature. Spiky structures in a low-energy region below 0.1 eV are due to the optical phonon modes. When the system undergoes the CO transition, the number of the optical phonon modes clearly increases. The activated phonon modes reflect the change of the crystal structure caused by the CO transition.

To quantify the phonon-spectral change, we show in Fig. 3 the optical conductivity spectra in a low-energy region below 0.1 eV which were deduced by the KK analysis of the reflectivity data shown in Fig. 2. The spectra at temperatures above T_{CO} show three sharp-peak structures due to the optical phonon modes which correspond to the external mode (0.02 eV), the bending mode (0.033 eV) and the stretching mode (0.07 eV), respectively.[14] The number of the phonon modes above T_{CO} is consistent with the cubic perovskite structure, although the perovskite structure in this compound is slightly distorted and have rhombohedral symmetry even at room temperature. The rhombohedral distortion is thus too small for any activated phonon modes to be observed in the metallic state above T_{CO}. Apparently the last two modes are subject to the large spectral change below T_{CO}, because these modes are more sensitive to the Fe-O lattice distortion than the external mode.[15] The breathing-type distortion of Fe-O octahedra may occur in the nominal Fe^{5+} site in the CO state to acquire the energy gain due to the crystal field.

Although all the phonon modes appear to be considerably affected by the CO transition, we focus our attention on the phonon spectra above 0.06 eV to avoid complexity in analysis.[16] The number of the peaks due to the phonon modes increases from one to two with decreasing temperature across T_{CO}. According to the CO model as shown in the inset to Fig. 2, the origin of the increase of the phonon modes can be attributed to the two reasons; (1) charge modulation (appearance of the new modes) and (2) anisotropy (splitting of the original modes). Modulation of the charge density has occurred along the pseudocubic $[111]_c$ direction. This modulation may fold the phonon branches along the corresponding direction in k space into the reduced Brillouin zone, then the new optical phonon modes arise at the Γ point. In addition to the above effect, the anisotropy lifts the threefold degenerated IR-active phonon modes of the cubic perovskite ($F_{1u}\rightarrow A_{2u}+E_u$) but the degree of distortion is perhaps too small to cause such a large splitting ($\sim$0.01 eV) of the phonon modes. To assign the symmetry, we cannot utilize polarized spectra since the sample in the CO state shows a multidomain structure.[11] However we can distinct the new modes due to the charge modulation by comparing the spectra of other compounds which have rhombohedral symmetry but undergo no CO transition in the low-temperature insulating region; such as low-temperature $LaCoO_3$ (Ref. 17) as well as $Sm_{1-x}Sr_xFeO_3$ or $Gd_{1-x}Sr_xFeO_3$ ($x=\frac{2}{3}$).[18] An activated phonon peak around 0.08 eV, hereafter called A peak, in the spectra below T_{CO} is one such peak, which originates from folding of the branch of the stretching mode. We can

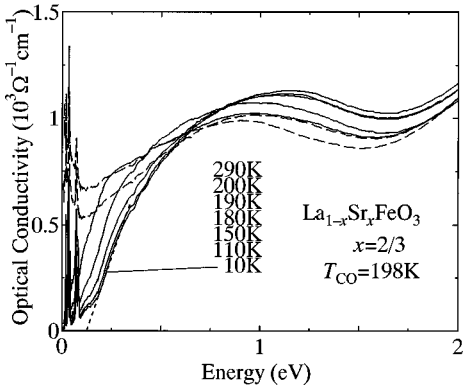

FIG. 4. Optical conductivity spectra below 2 eV at various temperatures for a $La_{1-x}Sr_xFeO_3$ ($x=\frac{2}{3}$) crystal with $T_{CO}=198$ K. Solid lines represent the spectra below T_{CO} and dashed lines represent the spectra above T_{CO}. A short dashed line is extrapolation of the onset of the 1-eV peak for the estimate of the magnitude of the optical gap energy at 10 K.

see only two modes perhaps relating to the stretching mode in Fig. 3 although folding due to the charge modulation of three times period may create two new Γ point modes. Thus, the A peak may consist of two A_{2u} modes which are nearly degenerate in frequency. The oscillator strength of the A peak must be related to the order parameter of the CO transition since it should be proportional to the amplitude of the lattice (perhaps breathing-type) distortion accompanied by the charge modulation. In order to estimate the oscillator strength, we have performed the conventional Drude and Lorentz curve fitting analysis by using the following formula:

$$\sigma(\omega)=\frac{\sigma_0}{1+(\omega\tau_0)^2}+\sum_{j=1}^{k}\frac{S_j\omega_j^2\gamma_j\omega^2}{(\omega_j^2-\omega^2)^2+\gamma_j^2\omega^2}. \qquad (1)$$

Here, σ_0 represents the dc conductivity, and τ_0 and $1/\gamma_j$ represent lifetime. ω_j and S_j are phonon frequency and oscillator strength, respectively. We assumed $k=4$ above T_{CO} and $k=8$ below T_{CO} for fitting (one of them is corresponding to a background part). Typical fitting curves are shown for the experimental spectra around the A peak at 290 and 10 K in the inset to Fig. 3. The calculated oscillator strength of the A peak and E peak (the original active mode around 0.07 eV) are shown in the third and the forth panel of Fig. 1. The value of the oscillator strength of the A (E) peak rises steeply at T_{CO}, slightly increases (decreases) and nearly saturates below 130 K with decreasing temperature. Discontinuous increase at T_{CO} suggests that this CO transition is the first-order transition. This is consistent with the existence of small temperature hysterisis of resistivity (a few K) around T_{CO}.

We show the optical conductivity spectra in an energy region between 0 and 2 eV in Fig. 4. The zero-frequency extrapolation of the spectrum is in accord with the dc conductivity value, which suggests that the electronic structure in this energy region must dominate dc transport mechanism as well. Overall features of the spectra have been discussed in Ref. 13 which reports on the systematic change of electronic structure at room temperature in $La_{1-x}Sr_xFeO_3$ with varying x. The 1-eV peak can be assigned to the CT-type transition between O $2p$ and Fe^{4+} e_g state, since its spectral weight is roughly proportional to the nominal hole doping x at the room temperature.[13,19] Above T_{CO} we can observe a clear Drude component below 0.1 eV, which signals the existence of the free carriers corresponding to a metallic value ($\sim 10^{-3}$ Ωcm) of the resistivity (see Fig. 1). As the temperature is decreased, Drude peak decreases its weight and the 1-eV peak becomes prominent. In the case of other CO systems such as Fe_3O_4 (Ref. 20) or $La_{2-x}Sr_xNiO_4$ ($x=0.33$),[21] a pseudogap feature was observed above T_{CO} due to the short-range order. However such a pseudogap is not clearly discernible in the present case.

Once the CO transition occurs, the spectral shape below 0.7 eV shows a drastic change that signals the evolution of the charge gap. Upon the CO transition, Drude peak is totally extinguished, a clear optical gap (2Δ) emerges, and the missing low-energy spectral weight is accumulated above 0.4 eV. The optical conductivity in the gap region rises almost linearly with the photon energy and shows a parallel shift to higher energy with decrease of temperature. The original spectral weight in the optical gap region is finally transferred above 0.7 eV and as a result the height of the CT peak grows with opening of the gap. This change of spectrum may be ascribed to the reconstruction of the electronic structure over an energy scale of the intersite coulomb repulsion. In other words, the optical gap has a character of the interatomic d-d transition, nominally $Fe^{3+}+Fe^{5+}\rightarrow Fe^{4+}+Fe^{4+}$, to which the hybridized O $2p$ states also contribute.

We tried to estimate the magnitude of the optical gap energy by extrapolating the onset part linearly to the base line of $\sigma(\omega)=0$, as shown by a dashed line for the 10 K spectrum. This approximate procedure cannot be accurate enough for the gap value itself because of the blurred tail feature and of its unknown theoretical shape, but can be a good quantitative measure of the gap opening because of the near-parallel shift of the conductivity onset. The result is shown in the bottom panel of Fig. 1. The value of 2Δ shows an onset at T_{CO}, increases sharply but continuously with decrease of temperature, and saturates at about 0.13 eV below 100 K. The temperature dependence seems to be of the BCS-type function that is predicted by the theory of the charge density wave/spin density wave transition.[22] However, the ratio of the gap energy (2Δ) to T_{CO} is about 7.6 which is twice as large as the theoretical value ($\sim$3.5) but half as small as in the quasi-2D case of $La_{2-x}Sr_xNiO_4$ ($x=0.33$).[21] The discrepancy between the theoretical and the experimental values may be attributed to the electron-correlation effect as in the $La_{2-x}Sr_xNiO_4$ ($x=0.33$) case.

One may notice in Fig. 1 that there is some difference between the temperature dependencies of the activated phonon intensity S_A (abrupt increase at T_{CO}) and the optical gap value (BCS-type temperature dependence), although both must be relevant to the order parameter of the charge-ordered phase. The intensity of the E peak in Fig. 3 (not activated by charge modulation) also shows a jump at T_{CO} and decreases with decreasing temperature (see Fig. 1).

This may be due to abrupt change of the effective charge of Fe ion. Thus, BCS-type temperature dependence of the gap value signals that the opening of the gap is governed not only by the charge modulation or associated lattice distortion

as measured by the phonon spectra, but also by the evolution of the staggered moment in the antiferromagnetic state. The CO transition occurs concurrently with the antiferromagnetic transition, as readily shown in Fig. 1. In fact, the magnetic susceptibility around T_{CO} shows a rather conventional cusp shape indicating the second-order-like magnetic transition.

In summary we have investigated the temperature dependence of optical conductivity spectra for the charge-ordering (CO) system $La_{1/3}Sr_{2/3}FeO_3$. As summarized in Fig. 1, resistivity increases steeply upon the CO transition and M/H shows a cusp at T_{CO} due to the antiferromagnetic order. Reflecting the periodic lattice distortion along the $[111]_c$ direction (in the pseudocubic setting) in the CO state, new phonon modes become infrared active, whose spectral intensity abruptly increases at T_{CO} and then shows weak temperature dependence. By contrast, the optical charge gap (0.13 eV in the ground state) rather continuously opens up with decrease of temperature below T_{CO}.

We are grateful to Y. Okimoto for fruitful discussions. This work was in part supported by a Grant-In-Aid from the Ministry of Education, Science, Sport, and Culture, Japan, and by the New Energy and Industrial Technology Development Organization (NEDO).

*Present address: Institute of Materials Science, University of Tsukuba 305-8573, Tsukuba, Japan.

[1] M. Imada, A. Fujimori, and Y. Tokura (unpublished).

[2] J. M. Tranquada, B. J. Sternlieb, J. D. Axe, Y. Nakamura, and S. Uchida, Nature (London) **375**, 561 (1995).

[3] Z. Jirak, S. Krupicka, Z. Simsa, M. Dlouha, and Z. Vratislav, J. Magn. Magn. Mater. **53**, 153 (1985).

[4] H. Kuwahara, Y. Tomioka, A. Asamitsu, Y. Moritomo, and Y. Tokura, Science **270**, 961 (1995).

[5] C. H. Chen, S.-W. Cheong, and A. S. Cooper, Phys. Rev. Lett. **71**, 2461 (1993).

[6] S.-W. Cheong, H. Y. Hwang, C. H. Chen, B. Batlogg, L. W. Rupp, Jr., and S. A. Carter, Phys. Rev. B **49**, 7088 (1994).

[7] Y. Moritomo, Y. Tomioka, A. Asamitsu, Y. Tokura, and Y. Matsui, Phys. Rev. B **51**, 3297 (1995).

[8] E. J. Verwey and P. W. Haayman, Physica (Amsterdam) **8**, 979 (1941).

[9] M. Takano and Y. Takeda, Bull. Inst. Chem. Res., Kyoto Univ. **61**, 406 (1983).

[10] P. D. Battle, T. C. Gibb, and P. Lightfoot, J. Solid State Chem. **84**, 271 (1990).

[11] J. Q. Li, Y. Matsui, S. K. Park, and Y. Tokura, Phys. Rev. Lett. **79**, 297 (1997).

[12] A. E. Bocquet, A. Fujimori, T. Mizokawa, T. Saitoh, H. Namatame, S. Suga, N. Kimizuka, Y. Takeda, and M. Takano, Phys. Rev. B **45**, 1561 (1992).

[13] S. K. Park, S. Yamaguchi, and Y. Tokura (unpublished).

[14] M. D. Fontana, G. Metrat, J. L. Servoin, and F. Gervais, J. Phys. C **17**, 483 (1984).

[15] S. Tajima, A. Masaki, S. Uchida, T. Matsuura, K. Fueki, and S. Sugai, J. Phys. C **20**, 3469 (1987).

[16] The 0.04-eV peak (the bending mode) is also strongly activated upon the CO transition. However, this mode can in principle be activated by a rhombohedral distortion, and hence not so appropriate for a quantitative measure for the symmetry-breaking inherent to the CO.

[17] S. Yamaguchi, Y. Okimoto, and Y. Tokura, Phys. Rev. B **55**, R8666 (1997).

[18] S. K. Park, T. Ishikawa, J. Q. Li, Y. Matsui, and Y. Tokura (unpublished).

[19] M. Abbate, F. M. F. de Groot, J. C. Fuggle, A. Fujimori, O. Strebel, F. Lopez, M. Domke, G. Kaindl, G. A. Sawatzky, M. Takano, Y. Takeda, H. Eisaki, and S. Uchida, Phys. Rev. B **46**, 4511 (1992).

[20] S. K. Park, T. Ishikawa, and Y. Tokura, Phys. Rev. B **58**, 3717 (1998).

[21] T. Katsufuji, T. Tanabe, T. Ishikawa, Y. Fukuda, T. Arima, and Y. Tokura, Phys. Rev. B **54**, R14 230 (1996).

[22] A. W. Overhauser, Phys. Rev. **128**, 1437 (1962); A. W. Overhauser, *ibid.* **167**, 691 (1968).